AIP Advances

Statistics of vacuum electrical breakdown clustering and the induction of follow-up breakdowns

Cite as: AIP Advances **12**, 115317 (2022); https://doi.org/10.1063/5.0111677
Submitted: 19 July 2022 • Accepted: 25 October 2022 • Published Online: 10 November 2022

Anders Korsbäck, Flyura Djurabekova and Walter Wuensch

Statistics of vacuum electrical breakdown clustering and the induction of follow-up breakdowns

Cite as: AIP Advances 12, 115317 (2022); doi: 10.1063/5.0111677
Submitted: 19 July 2022 • Accepted: 25 October 2022 •
Published Online: 10 November 2022

Anders Korsbäck,[1,a)] Flyura Djurabekova,[1] and Walter Wuensch[2]

AFFILIATIONS

[1] Helsinki Institute of Physics, University of Helsinki, P.O. Box 43, FI-00014 Helsinki, Finland
[2] CERN, European Organization for Nuclear Research, 1211 Geneva, Switzerland

[a)] Author to whom correspondence should be addressed: anders.korsback@helsinki.fi

ABSTRACT

Understanding the underlying physics of vacuum electrical breakdown is of relevance for the development of technologies where breakdown is of significance, either as an intended part of device operation or as a cause of failure. One prominent contemporary case of the latter is high-gradient linear accelerators, where structures must be able to operate with both high surface electric fields and low breakdown rates. Temporal clustering of breakdowns has for long been observed in accelerating structures. In this work, the statistics of breakdown clustering were studied using data collected by a system applying DC voltage pulses over parallel disk electrodes in a vacuum chamber. It was found that the obtained distributions of cluster sizes can be explained by postulating that every breakdown induces a number of follow-up breakdowns that are Poisson-distributed with $\lambda < 1$. It was also found that the primary breakdown rate, i.e., the breakdown rate after discounting follow-up breakdowns, fluctuates over time but has no discernible correlation with cluster size. Considered together, these results provide empirical support for the interpretation that primary and follow-up breakdowns are categorically different kinds of events with different underlying causes and mechanisms. Furthermore, they support the interpretation that there is an actual causal relationship between the breakdowns in a cluster rather than them simply being concurrent events with a common underlying cause.

I. INTRODUCTION

Vacuum electrical breakdown is the appearance of an electrically conductive plasma arc across an interelectrode vacuum gap, triggered by the application of a strong electric field on the electrode surface. Understanding the phenomenon is of importance for the development of devices that either use vacuum breakdown as part of their operation or whose operation is disrupted by breakdown. One prominent contemporary case of the latter is linear accelerators with a high accelerating gradient, whose cavities must be able to operate at high surface electric fields and low breakdown rates.[1–3] This has led to increased interest in breakdown research by the accelerator community in the last two decades.

While understanding of the mechanics of breakdown plasma ignition remains incomplete, the dominant view is that the dynamics of the breakdown are generally determined by the cathode, which provides the ions that constitute the plasma.[4] An initial population of ions could multiply by being accelerated back to the cathode and sputter more ions.[5–7] What causes the initial ejection of ions from the cathode is perhaps the least understood part and perhaps the most relevant part for finding ways to prevent breakdown. High local field emission current density has long been believed to be a part of the chain of events leading to breakdown,[8,9] and it has been observed in cathode surface scans as a precursor to breakdown.[10] Hence, it is possible that the initial ion population is produced by local evaporation on the cathode caused by the field emission current.[11–13] However, that in turn raises the question of what causes the high current density. The most common explanation is that surface protrusions cause geometric field enhancement.[11] However, such emission sites have been observed to dynamically appear and disappear under the application of electric field.[10] Hence, if the current is simply caused by geometric field

enhancement, there must be a microprocess where the electric field causes the shape of the surface to evolve, another subject of study in recent years.[14–17]

Breakdowns have an observed tendency to be clustered in time,[2,18,19] and recent research has shown that temporally clustered breakdowns also tend to be spatially clustered.[20,21] In a previous paper published by our collaboration, we introduced the concepts of primary and follow-up breakdowns.[20] Primary breakdowns are independent events that occur constantly at a low event rate. Follow-up breakdowns are breakdowns occurring at a higher event rate but only in the immediate aftermath of a preceding breakdown. This, together with the observed concurrent temporal and spatial clustering of breakdowns, led us to conclude that follow-up breakdowns are induced by preceding breakdowns. However, a reasonable alternative interpretation of the data would be that instead of the earlier breakdowns in a cluster causing the latter, they are all instead caused by some common underlying cause that temporarily and locally causes an elevated event rate.

In this paper, we further explore the statistics of breakdown clustering, particularly the distribution of cluster size. We do so in order to provide further support for our interpretation that primary and follow-up breakdowns are two different kinds of events in terms of underlying causes and mechanics and that there is indeed a causal relationship between the breakdowns in a cluster. In this paper, we only consider temporal clustering and not spatial clustering as the experimental setup used to collect the data used did not have the capability to localize breakdowns at the time of the experiments.

The experiments that this paper is based on were carried out at CERN in the DC Spark Lab. It is a facility and associated experimental effort established to be complementary to experiments using accelerating structures. By using voltages in the kilovolt range applied over gaps in a size range of tens of micrometres, it allows for breakdown experiments to be carried out at lower hardware cost and higher data collection throughput compared to experiments using accelerating structures. The experimental setup and methods used are sufficiently general that the results should be applicable beyond the field of accelerator technology. The data analyzed in this paper is partly reused data from previous experiments and partly new data, all of them treated with a novel focus on cluster size distribution.

II. EXPERIMENTAL METHODS

A. Measurement setup and process

All measurements were performed using the setup we have named as the large electrode DC spark system. It uses interchangeable disk electrodes, shown in Fig. 1, in a parallel surface (diameter 62 mm) geometry. The parallel geometry is ensured by stacking the electrodes together with a cylindrical insulating ceramic Al_2O_3 spacer in between, resting on a rim below the gap surface. The height of the spacer determines the size of the interelectrode gap, which was 60 μm in all experiments. All critical dimensions were manufactured to a tolerance of 1 μm. The edges of the top surface of the electrode are rounded (radius 1 mm) to mitigate field enhancement by the edge and to prevent breakdown through the spacer. All electrodes used in these experiments were made from 3D forged oxygen-free electronic copper, in accordance with the CERN standard for copper used for accelerating structures.[22]

FIG. 1. Electrode used by the large electrode system for breakdown experiments. A pair of such electrodes facing each other symmetrically forms the interelectrode vacuum gap. The spacer separating the electrodes rests on the outer rim of the bottom electrode, and in turn supports the top electrode by the rim.

The electrode-spacer stack is held in a vacuum chamber (10^{-11} bar), with voltage pulses applied through electrical feedthroughs. Voltage is provided by a DC power supply, charging a 200 m long coaxial cable used as a pulse-forming network. Square pulses of length in the μs range are applied from the cable over the electrodes by closing and opening a fast solid-state high voltage switch. Pulsing is controlled by a programmed microcontroller that provides the input signal for the switch and in turn communicates with a desktop computer, providing high-level control and data logging in LabVIEW.

Pulsing is performed at a constant rate of up to 1000 pulses per second, capped by power dissipation constraints at higher voltages. The microcontroller counts the number of applied pulses. Upon the occurrence of a breakdown, the DC supply voltage is cut off, and pulsing is paused for half a minute to allow for restoration of the vacuum. The breakdown drains the charge stored in the coaxial cable. The occurrence of the breakdown is logged by the system, together with the number of pulses that preceded it, thus providing a record of the total number of pulses applied and the points in the sequence of pulses when breakdowns happened.

Pulsing is resumed by a signal sent from the computer to the microcontroller, and a simultaneous signal that turns on the DC supply voltage is sent. This causes the charge and the voltage in the cable to rise asymptotically toward a set value, reaching 90% of the set value in about 700 ms and 99% of it in about 1400 ms. Thus, the voltage of the applied pulses is gradually ramped up in the aftermath of a breakdown.

As the system has already been described thoroughly elsewhere, we provide references to more detailed descriptions of the system, including a schematic of the circuit and a discussion of instrumentation issues and capabilities.[19,20,23,24]

B. Measurement runs

A total of six datasets produced by different measurement runs were used for the analysis in order to study breakdown clustering under varied conditions. The input parameters of the measurement

TABLE I. Input parameters and other properties of experiments producing the datasets. The voltage of dataset VI was feedback-controlled and fluctuated in the range 4.0–4.8 kV.

Dataset	I	II	III	IV	V	VI
Electrode type	Hard	Hard	Hard	Soft	Soft	Hard
Voltage (kV)	2.3	2.8	4.2	4.5	4.65	*
Pulse length (μs)	6.0	3.5	2.0	5.0	5.0	5.0
Number of breakdowns	30 108	1537	3200	2099	1578	3856
Number of pulses ($\times 10^6$)	784	139	87	404	64	296
Breakdowns per pulse ($\times 10^{-5}$)	3.84	1.10	3.69	0.52	2.47	1.30

runs and the number of pulses and breakdowns in the datasets are summarized in Table I.

Datasets I–III are the same as in the previous study of breakdown statistics,[20] labeled B–D, respectively. These were all run consecutively on the same electrode pair. This electrode pair was used as machined and thus of relatively hard copper. In this paper, we refer to this kind of electrode pair as "hard" for the sake of brevity. The system was set to run automatically at a set voltage and pulse length, applying voltage pulses and recording breakdowns as described in Sec. II A until a satisfactory amount of data had been collected or the setup was needed for other activities.

Datasets IV and V are new datasets collected for this study. They were collected using an electrode pair that had been subjected to heat treatments after machining, treatments identical to those used to bond accelerating structures together.[25] The treatments heat the electrodes almost to the melting point of copper, causing the copper to become soft and obtain a large grain size. We correspondingly refer to this kind of electrode pair as "soft." This electrode pair was previously used in our recent study on electrode breakdown performance conditioning,[26] where it was referred to as sample 3. This electrode pair was used for the present study because it had undergone extensive conditioning during the preceding experiment and was unlikely to condition further. As with datasets I–III, these datasets were also collected by letting the system run automatically at a set voltage and pulse length.

Dataset VI is the same as that in the study of breakdown conditioning,[26] where it was referred to as sample 2. This dataset was collected using a "hard" electrode pair, a different one from the one used to collect datasets I–III. Contrary to the other datasets, the pulse voltage was not held constant in this measurement run. Instead, as this measurement run was carried out as a part of our study of electrode conditioning, the voltage was controlled by a negative feedback loop in response to the breakdown behavior: The set value of voltage was reduced by up to 10 V if a breakdown happened within 20 000 pulses after the preceding breakdown and increased by 10 V if there was no breakdown during 100 000 consecutive pulses. As this was a pristine electrode pair, it spent the first 23×10^6 pulses conditioning before settling to fluctuate around a level of ultimate breakdown performance. This initial conditioning was excluded from the analysis in this paper. Thus, voltage fluctuated over the course of the measurement run, but the breakdown rate was largely constant due to negative feedback. The pulse length was also set to a constant value in this measurement run. The system ran automatically until then.

For a more detailed description of this measurement run and the feedback loop, please refer to the conditioning study.[26]

For further discussion on the differences in the material state and breakdown dynamics between electrodes of soft and hard copper, again refer to the conditioning study.[26]

III. RESULTS AND DISCUSSION

A. Breakdown classification

For each dataset, every breakdown was classified as either a primary or a follow-up breakdown. The classification was done based on statistical analysis of the number of pulses between two consecutive breakdowns.[20] The threshold number of pulses between breakdowns is determined for each dataset; every breakdown happening within that many pulses of the preceding breakdown is classified as a follow-up, and the remaining are classified as primary ones. The threshold is obtained from the probability density function of the number of pulses between breakdowns by fitting a sum of two exponential decreases to it. One of the two terms of the fit corresponds to primary breakdowns, and the other terms correspond to follow-up breakdowns. Thus, the relative magnitudes of the two terms for a given number of pulses between breakdowns give the probabilities of the second breakdown of the pair being either a primary or a follow-up. Thus, the number of pulses between breakdowns for which the terms are equal can be used as the aforementioned threshold value for classification.

This provides a reasonably accurate classification of breakdowns, with a significant risk of misclassification only for the number of pulses between breakdowns close to the threshold. For a more thorough discussion on the method of classification and for illustrating figures, please refer to the previous work.[20] Spatial localization of breakdowns could also be used to improve classification,[21] but this feature is not yet available for the datasets used in this paper.

The number of primary and follow-up breakdowns thus obtained is shown in Table II. The number of breakdowns of each type for datasets I–III differs slightly from that reported in the previous work[20] since the fit was made this time with a priority to define the threshold as accurately as possible rather than obtaining the best possible fit to the majority of the probability density functions.

B. Cluster size distribution

Having classified breakdowns into primary and follow-up breakdowns, we further study breakdown clustering. We define a

TABLE II. Number of primary and follow-up breakdowns in each dataset.

Dataset	I	II	III	IV	V	VI
Number of primary breakdowns	5 672	833	2105	1287	673	2799
Number of follow-up breakdowns	24 436	704	1095	812	905	1057
Total number of breakdowns	30 108	1537	3200	2099	1578	3856
Ratio follow-up breakdowns per primary	4.31	0.85	0.52	0.63	1.34	0.38

cluster as a series triggered by a primary breakdown and followed by subsequent follow-up breakdowns that occur until the next primary breakdown takes place. For the sake of brevity, we use "cluster" to also mean lone primary breakdowns without any follow-up ones.

Histograms of cluster sizes were calculated for each dataset, and attempts were made to find a function that fits the data. We found that the best possible fit was obtained by making the following postulate: Each breakdown (of either kind) induces a number of follow-up breakdowns that is Poisson-distributed with a constant $\lambda < 1$, that is, the probability that a breakdown induces exactly n follow-up breakdowns is

$$P(n) = \frac{\lambda^n e^{-\lambda}}{n!}. \quad (1)$$

The value of the parameter λ would depend on system-specific conditions such as voltage applied and energy released in a breakdown, with conditions that cause a higher likelihood of follow-up breakdowns resulting in a larger λ and larger clusters. The key point is that λ is constant throughout the cluster, i.e., every breakdown in a cluster would have an equal chance of inducing further breakdowns regardless of its place in the cluster. Thus, from our postulate, a general shape for the distribution of cluster size is one that holds regardless of the strength of the tendency for breakdowns to induce follow-up breakdowns. The requirement that $\lambda < 1$ is made to ensure that the cluster will eventually extinguish itself rather than continuously inducing follow-up breakdowns indefinitely.

Analytically deriving the probability mass function (PMF) of cluster size from Eq. (1) would be awkward; thus, it was instead obtained numerically through a Monte Carlo method. For each value of λ from 0.01 to 0.90 in increments of 0.01, a billion clusters were randomly generated to obtain the PMF of the cluster size for that particular value of λ. Each cluster was generated as follows: The cluster starts with a primary breakdown, and a random Poissonian number is generated to determine whether any follow-up breakdowns are induced. If the number is greater than zero, it gives the number of follow-up breakdowns in the first generation. For each of these, a Poissonian random number is likewise generated to determine the number of follow-up breakdowns in the next generation and so on in a cascade manner. This continues until a generation produces no further breakdowns. At this point, the total number of breakdowns in the cluster is tallied. PMFs for values of λ in between those tested for were obtained by interpolation.

From the PMFs thus obtained, the expected number of clusters of each size in a dataset is obtained by normalizing the PMF to the total number of clusters in the dataset. The normalized PMF was fit to the histograms, with λ being the sole fitting parameter. The fits were performed using Pearson's χ^2 test, finding the value of λ that minimizes the test statistic χ^2. The tail ends of the histograms where the expected number of clusters of a given size is less than 5 were excluded from the fit as the test breaks down for small expectation values.

Figure 2 shows the histograms of the cluster size along with the fits. Error bars show the expected binomial random variation (one standard deviation) around the expectation value. From the χ^2 value and the number of degrees of freedom (two less than the number of bins since there is one fitting parameter), p-values for each fit can be calculated. If the fit would be a perfect match with the underlying distribution, and thus if any difference between the fit and the data

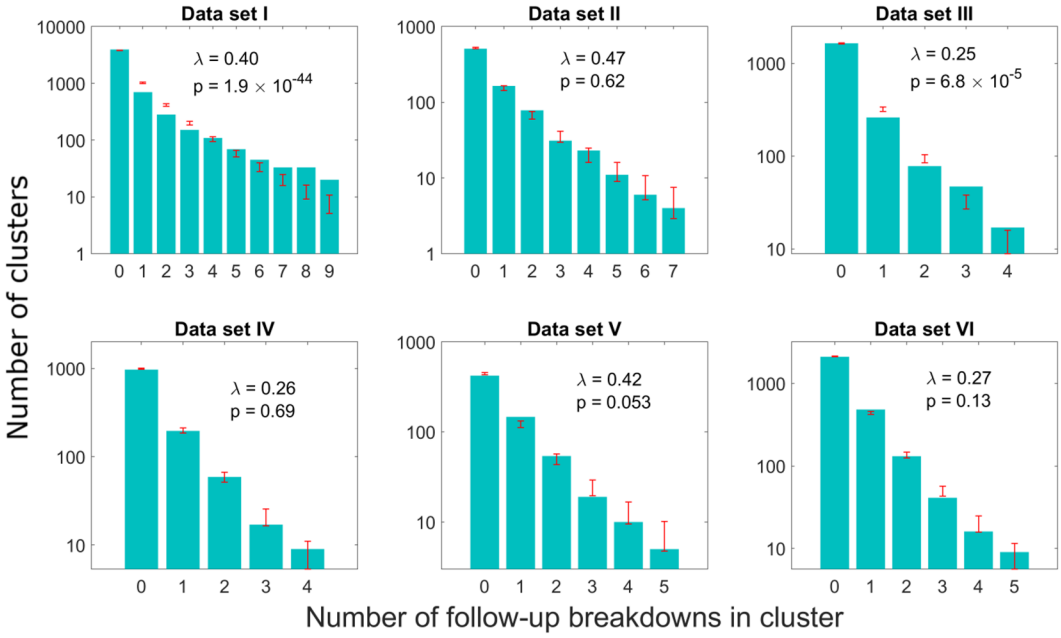

FIG. 2. Histograms showing the distributions of cluster sizes and fits of the (normalized) PDF. Histogram bars show the number of clusters of each size; red error bars show the fit and expected variation (one standard deviation) around the fit value.

TABLE III. Properties of fits to histograms of cluster size, datasets I–VI.

Dataset	I	II	III	IV	V	VI
Electrode type	Hard	Hard	Hard	Soft	Soft	Hard
Number of breakdowns	30 108	1537	3200	2099	1578	3856
Number of clusters	5 672	833	2105	1287	673	2799
Fit λ	0.40	0.47	0.25	0.26	0.42	0.27
Fit χ^2	226.2	4.40	21.91	1.47	9.34	7.20
Degrees of freedom	8	6	3	3	4	4
Fit p-value	1.9×10^{-44}	0.62	6.8×10^{-5}	0.69	0.053	0.13

TABLE IV. Properties of fits to histograms of cluster size, subsets of dataset I.

Subset	I.1	I.2	I.3	I.4	I.5
Number of clusters	614	1049	1019	2421	1008
Fit λ	0.75	0.51	0.24	0.08	0.45
Fit χ^2	11.23	12.05	13.52	17.00	26.16
Degrees of freedom	9	7	3	1	6
Fit p-value	0.26	0.10	0.0036	3.7×10^{-5}	2.1×10^{-4}

would be due to random variation, we would expect p-values for the fits to be uniformly distributed in the range 0–1. Thus, p-values for the fits provide an indication of how well our postulate fits the data. Table III shows the properties of the fits.

As we can see from Table III, the p-values are consistent with our postulate for datasets II and IV–VI. Visual inspection of Fig. 2 confirms this, with the histogram bin heights for these datasets being within or slightly outside the error bars. We think that the extent to which the data and the fits match is remarkable, considering how the bin heights vary over two to three orders of magnitude and how the fit is not particularly flexible but largely fixed by the first data point, as that point has the smallest relative error bars due to the law of large numbers.

For datasets I and III, we get p-values showing a statistically significant difference between the data and the fit. Visual inspection of Fig. 2 shows that the relative shape of the two is the same in both cases. The data are consistently below the fit at small cluster sizes and consistently above it at large cluster sizes. We also note that these two datasets are relatively large, being first and third in the number of both breakdowns and clusters, respectively. This led us to suspect that the discrepancy is due to λ fluctuating over time. In that case, the actual obtained distribution would become a superposition of distributions with different values of λ, with the value obtained from the fit being an average. We explored this possibility by doing subset analysis of dataset I and by numerically simulating experiments with fluctuating λ.

In our previous work on breakdown statistics,[20] subset analysis was performed on dataset I. The dataset was divided chronologically into five segments with the same number of breakdowns in each segment. It was shown that the primary, follow-up, and overall breakdown rates fluctuated over the course of the measurement run. Now we use the same subsets to study the fluctuation of the λ parameter. For each subset, a histogram of the cluster size was calculated, and a normalized PMF was fit to it in the same way as was done for datasets I through VI. The properties of the fits are shown in Table IV. As can be seen, λ does drift as hypothesized, starting at 0.75 for the first subset, then monotonically decreasing all the way to 0.08 for the fourth subset, and finally rebounding to 0.45 for the fifth. However, even with a unique value of λ for each subset, only two subsets out of five (the first and the second) yield p-values that indicate consistency between the data and the PMF.

The effect of a fluctuating λ on the distribution of cluster size was studied through simulation of the clustering process. During each iteration of the simulation, λ is given a random value uniformly distributed in the range 0.1–0.8, after which one cluster is generated using the same Monte Carlo method previously described. Then a new iteration starts, giving λ a new random value and generating a new cluster. Once a predetermined number of iterations have been run, a histogram of the cluster size is created, and the normalized PMF fit to it.

Figure 3 shows the cluster size distributions and PMF fits of two such simulations, one with 2000 and another with 20 000 generated clusters. We note that both have the same shape as datasets I and III in Fig. 2, with the data being consistently below the fit for small cluster sizes and above it for large cluster sizes. We also note that the values of λ provided by the fits are remarkably close to 0.45, the average of λ in the simulations. The difference in p-values shows how the difference between the data and the fit becomes increasingly statistically significant as the total number of clusters increases. As the simulation with 2000 clusters yielded a p-value in an order of magnitude close to the limit of statistical significance, we thought it warranted to briefly study the distribution of p-values obtained from this simulation. Hence, this simulation was repeated 100 times. Each of these 100 simulations produced a cluster size distribution, to which the normalized PMF was fit and a p-value was calculated. This set of p-values had a median of 0.0165, and 31 out of the 100 p-values were greater than 0.05. Considering this, it is entirely plausible that there is some fluctuation of λ in datasets II and IV–VI as well, but the effect and/or the sample sizes are too small to result in a statistically significant difference between the fit and the experimental data.

While the explanation that λ is variable could be considered an *ad hoc* hypothesis, there is some instrumentational justification for it, that is, after samples of the current design had been used for a number of experiments, it was found that the design is insufficient at mitigating the field enhancement effect of the electrode edge, particularly in a situation where the electrodes are parallel but misaligned off the centre. This results in a disproportionate number of breakdowns happening at the edges of the electrode. This tendency is most prominent in hard electrodes[26] but has also been occasionally observed in soft electrodes,[21] particularly in soft electrodes that have already undergone conditioning.[27] Breakdowns at or very close to the edge could plausibly have a lower λ than breakdowns far from the edge as there is less electrode surface in the vicinity of the breakdown site for new breakdown sites to appear at. This would result in a cluster size distribution that is a superposition of two PMFs with different values of λ. It is worth mentioning that the two datasets for which the fit and the data showed a statistically significant difference, i.e., I and III, were both collected with the same hard electrode

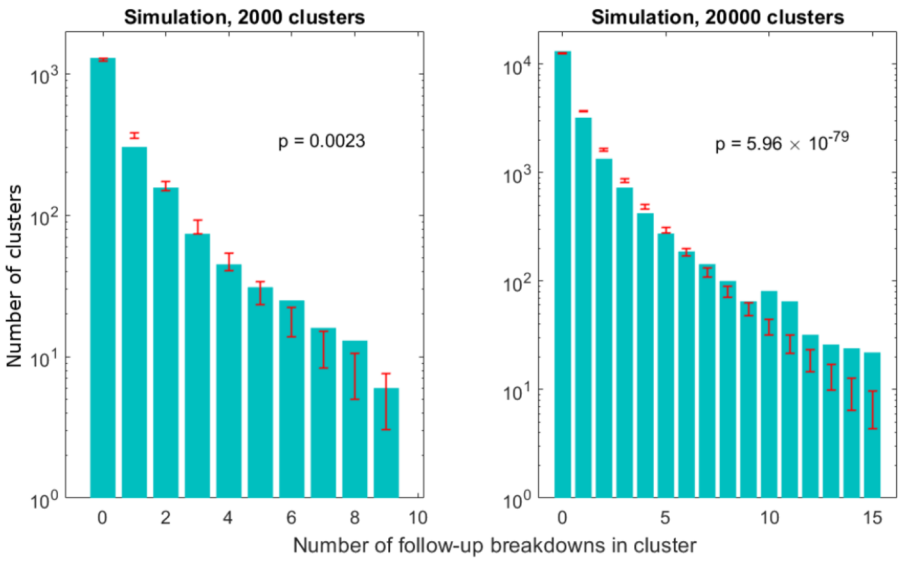

FIG. 3. Histograms of distributions of cluster sizes and simulations of clustering under conditions of fluctuating λ. Histogram bars show the number of clusters of each size, and red error bars show fit and expected variation (one standard deviation) around the fit value.

pair and thus would have had a high relative propensity to have edge breakdowns. Thus, the "variable λ" hypothesis is consistent with earlier experimental results. The existence of both edge and non-edge breakdowns would explain why we get cluster size distributions that are superpositions of PMFs with different values of λ but not why λ would drift over time as shown by the subset analysis of dataset I. However, as samples are known to undergo dynamic changes over the course of their operation in a way that affects their breakdown behavior,[20,26,28] it is not unreasonable to conjecture that the conditions that determine λ would also change over time, or that breakdown activity would move between regions of low and high λ.

C. Evolution of the primary breakdown rate and cluster size

In Sec. III B, we showed how the distribution of cluster size is consistent with the hypothesis that clustering is caused by breakdowns, triggering a cascade of further breakdowns. If this hypothesis is true, it would follow that the micromechanics of the process that leads to breakdown are at least partly different for primary and follow-up breakdowns. In other words, an effect that facilitates the occurrence of follow-up breakdowns should not be present in the process leading up to a primary breakdown. Furthermore, breakdown rates have been observed to fluctuate over time.[20,26,28] This warrants a comparative study of the evolution of the primary breakdown rate and cluster size. If primary and follow-up breakdowns are different kinds of events with different underlying micromechanics, one would expect the primary breakdown rate (in terms of the average number of pulses between subsequent clusters) and cluster size to be uncorrelated. However, if the two kinds of breakdowns actually are of the same kind with a single fluctuating event rate and clustering is simply a result of the underlying mechanisms being activated particularly strongly at certain times, one would reasonably expect the primary breakdown rate and cluster size to be positively correlated. Thus, it is of interest to explore whether there is such a correlation, and that is what we do in this subsection.

Figure 4 shows the evolution of the average number of follow-up breakdowns per cluster against the primary breakdown rate. Each point is calculated from a given number of consecutive primary breakdowns and their clusters. The number of clusters per point was chosen for the convenience of data visualization and varied from 10 to 100 depending on the dataset. The connecting jagged lines show the order of the points and thus the relative time-evolution of the primary breakdown rate and the average number of follow-up clusters. Breaks in the line appear where the average number of follow-up breakdowns goes to zero and cannot be shown on a logarithmic plot. For dataset VI, this analysis is less relevant than for the others as the two plotted quantities are causally related through the feedback loop that controls the pulsing voltage, but it is nevertheless included in the analysis for the sake of completeness.

Simple visual inspection of the plots suggests that there is little to no correlation between the two plotted quantities and that both quantities have a certain persistence to them, both drifting independently of each other. To further explore whether this is the case, we conducted a covariance study. Cross-covariance is the degree of correlation between two time-series as a function of the difference in time between them, where the time difference is called lag (τ). Autocovariance is the cross-covariance between a variable and itself and thus indicates how persistent its value is over time. In our case, we compare primary breakdown rates and cluster sizes at the points in time when clusters occur, rather than continuously over time. Hence, our measure of lag will be the number of clusters rather than time. Thus, we obtain the following definitions for autocovariance and cross-covariance, respectively:

$$K_{XX}(\tau) = E(X_i X_{i+\tau}) - \mu_x^2,$$
$$K_{XY}(\tau) = E(X_i Y_{i+\tau}) - \mu_x \mu_y, \quad (2)$$

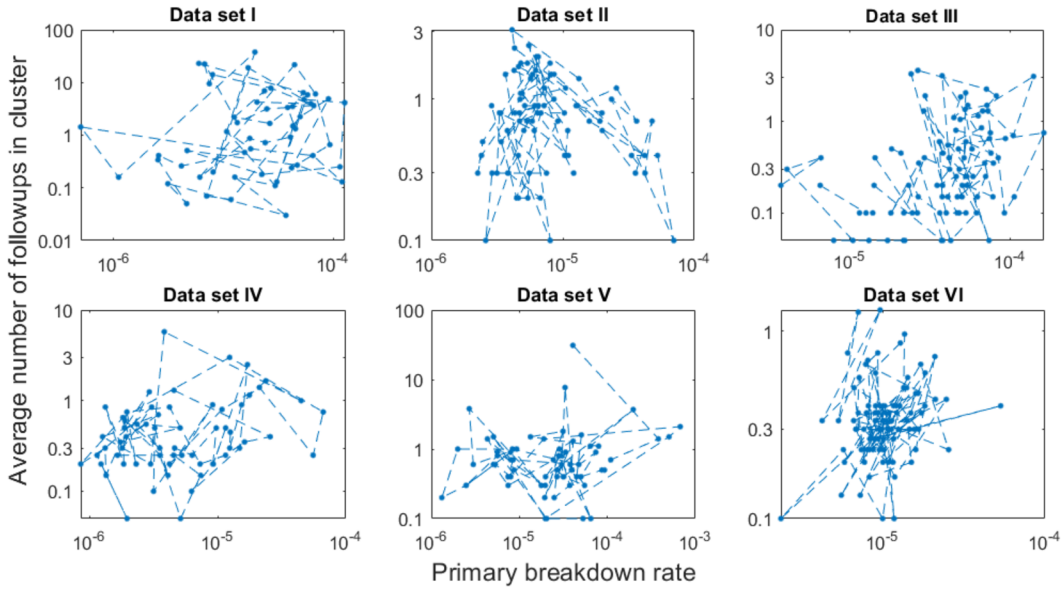

FIG. 4. Evolution of the primary breakdown rate and the average number of follow-up breakdowns per cluster.

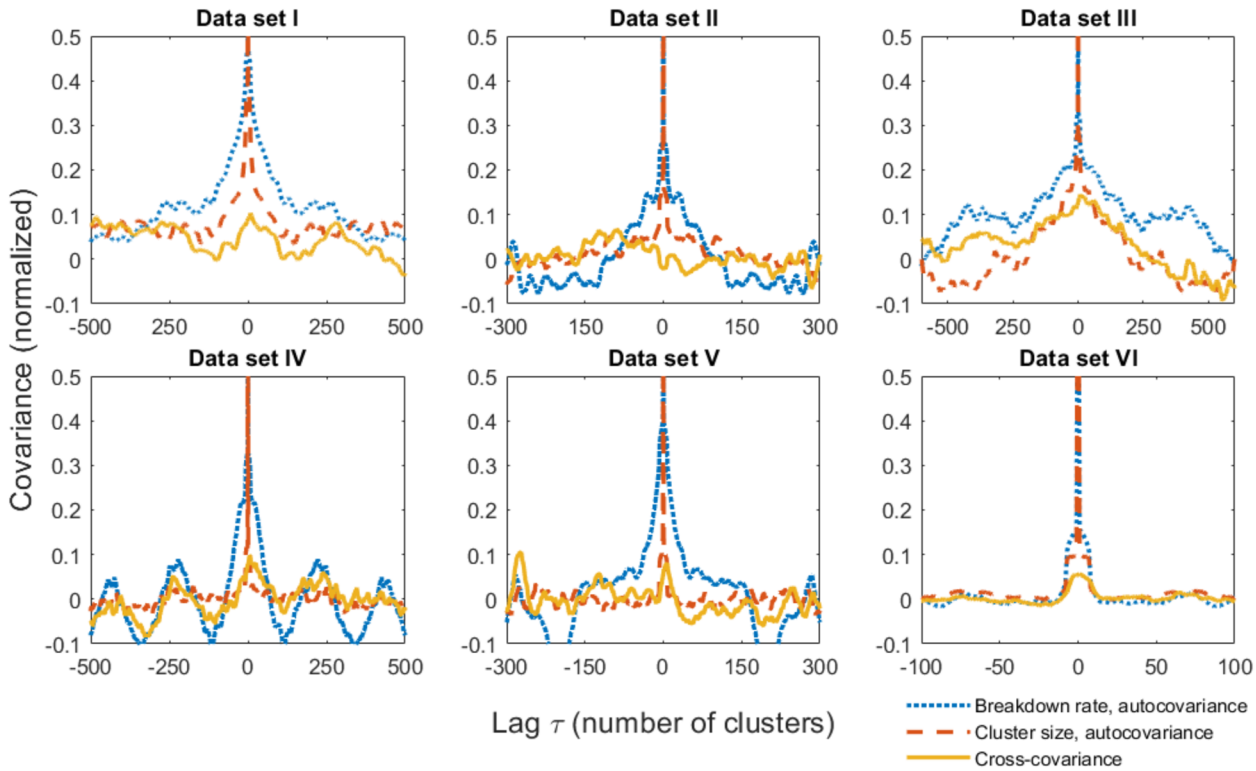

FIG. 5. Autocovariance of the primary breakdown rate (dotted blue line) and cluster size (dashed red line) and their cross-covariance (solid yellow line). The lines shown are smoothed by a moving average for the sake of legibility.

where X_i and Y_i are variable values at the ith cluster in the dataset, μ_x and μ_y are the respective mean values of the variables, and E is the expectation value function averaging over all possible pairs of clusters that are τ apart.

The time series of the cluster size and primary breakdown rate were constructed, with each time series element being derived from one cluster (i.e., elements were in chronological order but not equally spaced in time). Cluster size is simply the number of breakdowns in the cluster. The primary breakdown rate is the inverse of the number of pulses between the primary breakdown of the cluster and the preceding breakdown (i.e., the last breakdown of the preceding cluster). As both primary breakdown rate and cluster size are distributed over several orders of magnitude, we used the tenth logarithms of both in order to mitigate the effect of outliers. Because of this, we use cluster size here rather than the number of follow-up breakdowns in a cluster as the latter can have a value of zero, whose logarithm is undefined. Using Eq. (2), autocovariances and cross-covariance were calculated from these time series. The obtained covariances were further normalized so that autocovariances are equal to one at $\tau = 0$ in order to make them comparable to each other.

Figure 5 shows the resulting autocovariances and cross-covariances. Dataset VI shows little of either, as expected, due to the voltage control feedback loop; thus, we will exclude it from the discussion. For all the other datasets, we see that the autocovariance of the primary breakdown rate has a relatively wide peak around zero lag, with a width of ±50 to 200 clusters. Hence, the primary breakdown rate definitely has persistence, and this number of 50–200 primary breakdowns is indicative of the time scale of fluctuation. Curiously, the primary breakdown rate even shows periodicity in dataset IV, although that is a topic beyond the scope of this paper. The results regarding autocovariance of cluster size are much more mixed. Datasets I and III show a clear peak around zero, dataset II is a small one at most, and datasets IV and V are none at all beyond $\tau = 0$. This seemingly inconclusive result is, however, consistent with the variable λ hypothesis we presented in Subsection III B. Datasets I and III are the two that show a statistically significant discrepancy between the actual cluster size distribution and the distribution following from our hypothesis. If λ drifts over time, that would give average cluster size persistence and make it drift along with λ. Thus, the obtained autocovariances of cluster size support the interpretation that datasets I and III have a drifting λ and the other datasets do not. Finally, we note that cross-covariance of the breakdown rate and cluster size has a peak that visibly rises above the level of random fluctuation only in the case of dataset III, that is, even for dataset I for which the two are persistent, there is no clear correlation between the two, but they drift independently of each other. Considering how dataset III is unique in this regard, it is entirely possible and even reasonable to conjecture that it is a case of spurious correlation of two persistent quantities happening to drift in the same direction more often than in the opposite and thus appearing correlated.

All things considered, we can conclude that the primary breakdown rate does drift over time but has little to no effect on breakdown clustering or at most has so in very specific situations that might be experimental artifacts. This supports the interpretation that primary and follow-up breakdowns are two different kinds of events with different causes leading up to them.

IV. CONCLUSIONS

We have explored the temporal clustering of breakdowns. We have shown that the statistics of breakdown clustering support the interpretation that clustering is caused by breakdowns inducing further breakdowns. This has generally been the working assumption in the breakdown research community, but evidence for it has been scarce and circumstantial. Thus, this result is more of a confirmation of what is already believed than a new discovery. Nevertheless, it serves to fill a gap in the body of empirical evidence in favor of the prevailing view.

We have shown that the distribution of cluster size can be explained to a reasonable degree by postulating that every breakdown induces a number of follow-up breakdowns that are Poisson-distributed with an expectation value $\lambda < 1$. One significant implication of this is that there is a critical point at $\lambda = 1$, above which each breakdown induces an average of more than one more breakdown, and there is a risk of a runaway process of breakdowns inducing an ever-increasing number of further breakdowns.

The existence of this critical point provides an explanation for the "hot cell" phenomenon known in the high-grade accelerator community. This is the sudden occurrence of a very high breakdown rate inside one cell of an accelerating structure. It follows from our results that if one has an objective of preventing such a runaway process or to run a device at the highest possible field strength without causing one, the key is to monitor the clustering behavior (e.g., using λ as a key metric) rather than the overall breakdown rate, as has been the usual practice in the accelerator field.

As our results provide an explanation for the phenomena observed in diverse applications prone to breakdown behavior, there is reason to believe that our results are to some extent general and not limited to our experimental setup. This is particularly true for the qualitative results that there is a causal relationship between the breakdowns in a cluster and that there is a critical point after which the aforementioned runaway process occurs. The exact shape of the distribution of cluster size could, however, plausibly vary depending on the specifics of the system if there are circumstances that interfere with the induction of further breakdowns.

AUTHOR DECLARATIONS

Conflict of Interest

The authors have no conflicts to disclose.

Author Contributions

Anders Korsbäck: Conceptualization (equal); Data curation (equal); Formal analysis (equal); Investigation (equal); Methodology (equal); Software (equal); Validation (equal); Visualization (equal); Writing – original draft (equal); Writing – review & editing (equal). **Flyura Djurabekova**: Supervision (equal); Writing – review & editing (supporting). **Walter Wuensch**: Project administration (equal); Resources (equal); Supervision (supporting).

DATA AVAILABILITY

The data that support the findings of this study are available from the corresponding author upon reasonable request.

REFERENCES

[1]C. Adolphsen, W. Baumgartner, K. Jobe, F. Le Pimpec, R. Loewen, D. McCormick, M. Ross, T. Smith, J. Wang, and T. Higo, "Processing studies of X-band accelerator structures at the NLCTA," in *Proceedings of the 2001 Particle Accelerator Conference* (IEEE, Chicago, IL, 2001), Vol. 1, pp. 478–480.

[2]C. Adolphsen, "Normal-conducting RF structure test facilities and results," Technical Report No. SLAC-PUB-9906, SLAC, 2003.

[3]M. Aicheler, P. Burrows, M. Draper, T. Garvey, P. Lebrun, K. Peach, N. Phinney, H. Schmickler, D. Schulte, N. Toge *et al.*, "A multi-TeV linear collider based on CLIC technology: CLIC conceptual design report," Technical Report No. CERN-2012-007, CERN, 2012.

[4]A. Anders, *Cathodic Arcs: From Fractal Spots to Energetic Condensation* (Springer Science & Business Media, 2009), Vol. 50.

[5]H. Timko, K. Matyash, R. Schneider, F. Djurabekova, K. Nordlund, A. Hansen, A. Descoeudres, J. Kovermann, A. Grudiev, W. Wuensch *et al.*, "A one-dimensional particle-in-cell model of plasma build-up in vacuum arcs," Contrib. Plasma Phys. **51**, 5–21 (2011).

[6]H. Timkó, "Modelling vacuum arcs: From plasma initiation to surface interactions," Ph.D. thesis, University of Helsinki, 2011.

[7]H. Timko, K. N. Sjobak, L. Mether, S. Calatroni, F. Djurabekova, K. Matyash, K. Nordlund, R. Schneider, and W. Wuensch, "From field emission to vacuum arc ignition: A new tool for simulating copper vacuum arcs," Contrib. Plasma Phys. **55**, 299 (2014).

[8]R. P. Little and W. T. Whitney, "Electron emission preceding electrical breakdown in vacuum," J. Appl. Phys. **34**, 2430–2432 (1963).

[9]P. A. Chatterton, "A theoretical study of field emission initiated vacuum breakdown," Proc. Phys. Soc. **88**, 231 (1966).

[10]E. V. Nefyodtsev, S. A. Onischenko, D. I. Proskurovsky, and A. V. Batrakov, "Observation of pre-breakdown emission sites and breakdowns of vacuum gaps under short-pulsed testing," IEEE Trans. Dielectr. Electr. Insul. **18**, 929–936 (2011).

[11]F. M. Charbonnier, C. J. Bennette, and L. W. Swanson, "Electrical breakdown between metal electrodes in high vacuum. I. Theory," J. Appl. Phys. **38**, 627–633 (1967).

[12]S. Parviainen, F. Djurabekova, H. Timko, and K. Nordlund, "Electronic processes in molecular dynamics simulations of nanoscale metal tips under electric fields," Comput. Mater. Sci. **50**, 2075–2079 (2011).

[13]A. Kyritsakis, M. Veske, K. Eimre, V. Zadin, and F. Djurabekova, "Thermal runaway of metal nano-tips during intense electron emission," J. Phys. D: Appl. Phys. **51**, 225203 (2018).

[14]A. S. Pohjonen, S. Parviainen, T. Muranaka, and F. Djurabekova, "Dislocation nucleation on a near surface void leading to surface protrusion growth under an external electric field," J. Appl. Phys. **114**, 033519 (2013).

[15]M. Veske, S. Parviainen, V. Zadin, A. Aabloo, and F. Djurabekova, "Electrodynamics—molecular dynamics simulations of the stability of Cu nanotips under high electric field," J. Phys. D: Appl. Phys. **49**, 215301 (2016).

[16]A. Kyritsakis, E. Baibuz, V. Jansson, and F. Djurabekova, "Atomistic behavior of metal surfaces under high electric fields," Phys. Rev. B **99**, 205418 (2019).

[17]V. Jansson, E. Baibuz, A. Kyritsakis, S. Vigonski, V. Zadin, S. Parviainen, A. Aabloo, and F. Djurabekova, "Growth mechanism for nanotips in high electric fields," Nanotechnology **31**, 355301 (2020).

[18]T. Shioiri, T. Kamikawaji, K. Yokokura, E. Kaneko, I. Ohshima, and S. Yanabu, "Dielectric breakdown probabilities for uniform field gap in vacuum," in *Proceedings ISDEIV. 19th International Symposium on Discharges and Electrical Insulation in Vacuum* (IEEE, Xian, China, 2000), Vol. 1, pp. 17–20.

[19]N. C. Shipman, "Experimental study of DC vacuum breakdown and application to high-gradient accelerating structures for CLIC," Ph.D. thesis, The University of Manchester, Manchester, UK, 2015.

[20]W. Wuensch, A. Degiovanni, S. Calatroni, A. Korsbäck, F. Djurabekova, R. Rajamäki, and J. Giner-Navarro, "Statistics of vacuum breakdown in the high-gradient and low-rate regime," Phys. Rev. Accel. Beams **20**, 011007 (2017).

[21]A. Saressalo, A. Kyritsakis, F. Djurabekova, I. Profatilova, J. Paszkiewicz, S. Calatroni, and W. Wuensch, "Classification of vacuum arc breakdowns in a pulsed DC system," Phys. Rev. Accel. Beams **23**, 023101 (2020).

[22]S. Sgobba and F. Leaux, "Cu-OFE bars/blanks/ingots," Technical Report No. 2001, EDMS No. 790779, CERN, 2015, https://edms.cern.ch/document/790779/6.

[23]J. Kovermann, "Comparative studies of high-gradient rf and DC breakdowns," Ph.D. thesis, RWTH Aachen University, 2011.

[24]R. Soares, W. Wuensch, J. Kovermann, S. Calatroni, and M. Barnes, "A 12 kV, 1 kHz, pulse generator for breakdown studies of samples for CLIC RF accelerating structures," in *Proceedings of IPAC2012 1205201* (International Particle Accelerator Conference, 2012), p. THPPC061.

[25]J. W. Wang, J. Lewandowski, J. Van Pelt, C. Yoneda, G. Riddone, D. Gudkov, T. Higo, T. Takatomi *et al.*, "Fabrication technologies of the high gradient accelerator structures at 100 MV/m range," in *IPAC10* (International Particle Accelerator Conference, Kyoto, Japan, 2010), p. THPEA064.

[26]A. Korsbäck, F. Djurabekova, L. M. Morales, I. Profatilova, E. R. Castro, W. Wuensch, S. Calatroni, and T. Ahlgren, "Vacuum electrical breakdown conditioning study in a parallel plate electrode pulsed DC system," Phys. Rev. Accel. Beams **23**, 033102 (2020).

[27]I. Profatilova, X. Stragier, S. Calatroni, A. Kandratsyeu, E. Rodriguez Castro, and W. Wuensch, "Breakdown localisation in a pulsed DC electrode system," Nucl. Instrum. Methods Phys. Res., Sect. A **953**, 163079 (2020).

[28]A. Grudiev and W. Wuensch, "Design of the CLIC main linac accelerating structure for CLIC conceptual design report," in *Proceedings of LINAC2010* (XXV Linear Accelerator Conference, Tsukuba, Japan, 2010), pp. 211–213.